

Instability of quasi-liquid on the edges and vertices of snow crystals

Kanako T. Sato*

*Department of Pure and Applied Sciences,
University of Tokyo, Komaba 3-8-1,
Meguro-ku, Tokyo 153-8902, Japan*

(Dated: November 5, 2018)

Abstract

In this paper, we show theoretically that there exists quasi-liquid on the edges and vertices of snow crystals between -4°C and -22°C , while the faces (0001) and (10 $\bar{1}$ 0) have no quasi-liquid layers. Investigating the macroscopic theory of quasi-liquid and applying to the edges and vertices of the crystal, we find that the quasi-liquid becomes unstable above the critical supersaturation point, which is above the water saturation point. The thickness of this unstable quasi-liquid layer continues growing indefinitely. We interpret this behavior as corresponding to continuous production and overflow onto neighboring faces in a real system. We hypothesize that the unstable growth of snow crystals originates from the edges and vertices, and it is due to the overflow of quasi-liquid from the edges and vertices onto the neighboring faces, which are rough and lack quasi-liquid. Our hypothesis accounts for the qualitative behavior of the relations between the morphological instability and the water saturation in the snow phase diagram.

PACS numbers: 81.10.Aj, 68.60.-p, 64.70.-p

*Electronic address: kana@jiro.c.u-tokyo.ac.jp

I. INTRODUCTION

The snow crystal is one of the most beautiful things in nature, and it has attracted human interest since long ago. Its basic form is a hexagonal prism bounded by two basal (0001) and six prism faces ($10\bar{1}0$). Nakaya [1] was the first to successfully produce snow crystals in the laboratory, and he investigated the relations between growth forms and experimental conditions (i.e., temperature and supersaturation relative to ice). Since his work, many experimental studies have been carried out [2]. The snow phase diagrams obtained in these studies exhibit two important features (See Fig.1). One is that three transitions occur in the basic crystal form: at temperatures near -4°C (plates to columns), -10°C (columns to plates), and -22°C (plates to columns). These transitions correspond to changes in the growth rates of the faces (0001) and the faces ($10\bar{1}0$) with temperature [3]. The second important point is that a morphological instability arises when the supersaturation relative to ice becomes sufficiently large. Especially above the water saturation point (saturation relative to supercooled water), the crystal growth originates from the edges and the vertices, and as a result, needles and sheaths are produced between -4°C and -10°C , and dendrites and sectors are produced between -10°C and -22°C .

The basic growth form of snow crystals is determined by the most slowly growing faces. The basal (0001) and prism ($10\bar{1}0$) faces grow slowly and become the bounding faces of the crystal. Assuming that the faces grow through the spreading motions of two-dimensional nuclei [4], and taking into account the vapor diffusion field surrounding the crystal, Frank proposed a possible explanation of the dendritic growth of snow crystals [5]. Based on the same idea, Yokoyama and Kuroda [6] simulated the growth of an infinitely long hexagonal column (i.e. a two-dimensional snow crystal), and they succeeded in showing that six primary branches are produced from the vertices of the column. The instability that results in the production of these branches is due to the nonuniformity of the vapor density surrounding the polyhedron crystal. Their simulation, however, also showed that when secondary branches are produced, the size of the primary branches becomes comparable with that of the original hexagonal column. This is not a realistic modeling of the dendrites in actual snow crystals. Furthermore, this theory cannot account for the snow phase diagram discussed above. It is thus apparent that we must take into account other, yet unknown effects to explain the dendritical instability.

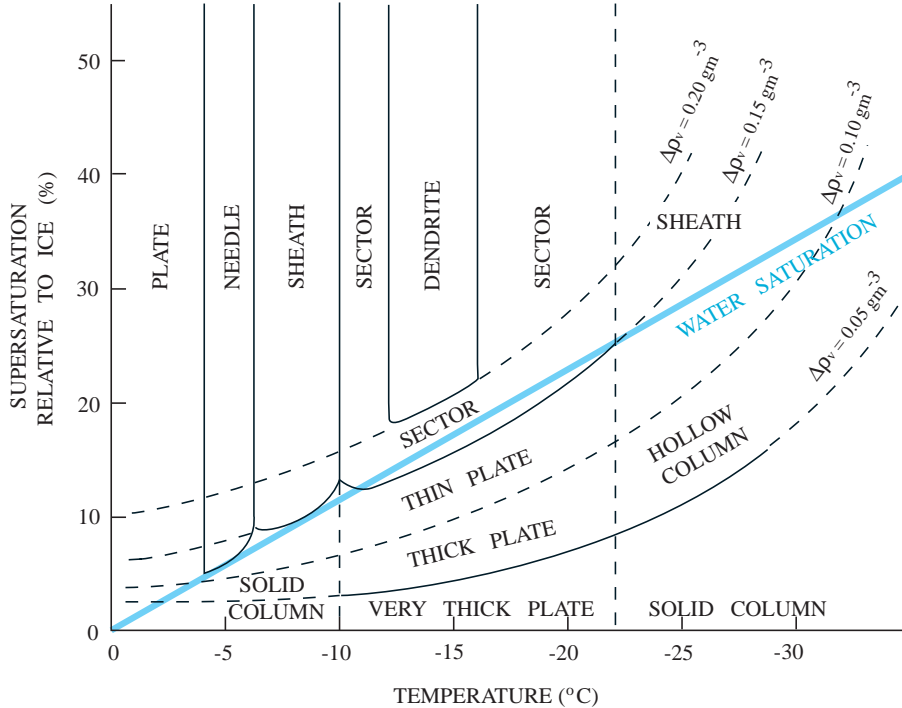


FIG. 1: Variation of ice crystal form with temperature and supersaturation. Here $\Delta\rho_v$ is the vapor density excess. (Based on laboratory observations [2].)

The three experimentally observed transitions in the basic crystal form at low supersaturation were accounted by the theory of Kuroda and Lacmann [11]. This theory is based on the well-known fact that the surface of ice existing just below 0°C is coated with a thin liquid like layer (quasi-liquid layer). This quasi-liquid layer has been observed using a variety of experimental techniques [13, 14, 15, 16, 17, 18, 19]. Theoretically, Weyl [8] gave qualitative arguments for its existence, and Fletcher [9] developed Weyl's arguments into a quantitative form. The starting point of Kuroda and Lacmann is a phenomenological model of the quasi-liquid layer proposed by Lacmann and Stranski [10]. On the basis of this model, Kuroda and Lacmann predicted that there exists quasi-liquid on the face $(10\bar{1}0)$ at lower temperatures than on the face (0001) . Recently, it has been observed in both experiments [16, 18] and molecular dynamics simulations [20] that there is a difference in behaviour of the quasi-liquid layer on basal and prism faces. Kuroda and Lacmann hypothesized that the surface structure of ice changes with decreasing temperature from a surface covered with

a quasi-liquid layer to a rough surface without a quasi-liquid layer and finally to a smooth surface. According to their description, the changes in crystal form are due to the anisotropy in these surface structural transitions between basal and prism faces of ice.

In this paper, we investigate the interaction between the quasi-liquid and the edges and vertices of snow crystals, whose growth originates from the edges and the vertices from -4°C to -22°C and above the water saturation point. In Section 2, we present a macroscopic model of a quasi-liquid layer and the explanation of the crystal form transitions proposed by Kuroda and Lacmann. In Section 3, we give an argument asserting that quasi-liquids remain on the edges and vertices in the temperature region between -4°C and -22°C , where the faces (0001) and $(10\bar{1}0)$ have no quasi-liquid layer. In Section 4, to examine curvature effects on the quasi-liquid, we investigate a model of an ice particle covered with a quasi-liquid layer in a vapor environment. In Section 5, we construct a macroscopic model describing a snow crystal whose six prism faces are without quasi-liquid but whose edges are covered with quasi-liquid. Using this model, we show that a novel instability arises on the edges and the vertices above the water saturation point due to the presence of the quasi-liquid. In Section 6, we present a new description of the relation between morphological instability and water saturation in the snow phase diagram. In Section 7, we give a summary.

II. QUASI-LIQUID LAYER ON A FLAT SURFACE

A quasi-liquid layer can exist in a stable state because its presence reduces the surface free energy of the system. The energetic advantage of surface melting is represented by $\Delta\sigma$ [10], defined as

$$\Delta\sigma = \sigma_{\text{vs}} - \sigma_{\text{sl}} - \sigma_{\text{lv}}, \quad (1)$$

where σ_{vs} is the surface energy per unit area of a vapor-solid interface, σ_{sl} that of a solid-liquid one, and σ_{lv} that of a liquid-vapor one. This parameter is positive for a system of water and ice, and thus in this case the existence of the quasi-liquid lowers the surface energy. The free energy per unit area of a quasi-liquid layer of thickness δ is given by [10, 11]

$$\Delta G_{\text{plane}}(\delta) = \sigma_{\text{lv}} + \sigma_{\text{sl}} + \Delta\sigma W(\delta) + \frac{\delta}{V_{\text{q}}}(\mu_{\text{l}} - \mu_{\text{s}}), \quad (2)$$

where V_{q} is the molecular volume in the quasi-liquid layer and μ_{l} and μ_{s} are the chemical potentials per molecule for the bulk liquid and the bulk solid, respectively. Here the function

$W(\delta)$ must satisfy the conditions $W(0) = 1$ and $W(\infty) = 0$, which result from the conditions $\Delta G_{\text{plane}}(0) = \sigma_{\text{vs}}$ and $\Delta G_{\text{plane}}(\infty) = \sigma_{\ell\text{v}} + \sigma_{\text{s}\ell} + \delta(\mu_{\ell} - \mu_{\text{s}})/V_{\text{q}}|_{\delta=\infty}$. To this time, two types of $W(\delta)$ have been used (see, for example, Ref.[21]). One is short range, $W_{\text{S}}(\delta) = \exp(-\delta/A)$, and the other is long range, $W_{\text{L}}(\delta) = (1 + \delta/A)^{-n}$ [11], where n is a positive integer ($n = 2$ for the Van der Waals forces [11]) and A is a parameter corresponding to the characteristic interaction length of the molecule in the quasi-liquid. Applying the minimization condition $\partial\Delta G_{\text{plane}}/\partial\delta = 0$, we find that the equilibrium thickness of the quasi-liquid layer is

$$\delta_{\text{eq}}^{\text{S}} = -A \ln \left(\frac{AQ_{\text{m}}(T_{\text{m}} - T)}{\Delta\sigma V_{\text{q}} T_{\text{m}}} \right), \quad (3)$$

for $W(\delta) = W_{\text{S}}(\delta)$, and

$$\delta_{\text{eq}}^{\text{L}} = -A + \left(nA^n \Delta\sigma V_{\text{q}} \frac{T_{\text{m}}}{Q_{\text{m}}(T_{\text{m}} - T)} \right)^{\frac{1}{n+1}}, \quad (4)$$

for $W(\delta) = W_{\text{L}}(\delta)$, where Q_{m} is the energy of melting per molecule, T is the absolute temperature, and T_{m} is the melting temperature. Here, we have used the equation $\mu_{\ell} - \mu_{\text{s}} = Q_{\text{m}}(T_{\text{m}} - T)/T_{\text{m}}$, which is derived from the Gibbs-Duhem relation assuming constant pressure and small $T_{\text{m}} - T$. As seen in Eqs.(3) and (4), the thickness of the quasi-liquid layer decreases monotonically with falling temperature. The above equations should be considered valid only until the thickness becomes on the order of a few monolayers, but beyond this point, we can consider the layer to have vanished. At this temperature, the surface strongly adsorbs H_2O molecules, and it thus become rough at the molecular level. The number of adsorbed molecules decreases with falling temperature, until eventually it vanishes, and the surface is thus smooth.

The parameter $\Delta\sigma$ can be approximated in terms of the number density of the broken bonds per unit area ρ as

$$\Delta\sigma = \frac{1}{2}\rho \left(\frac{Q_{\text{s}}}{N_{\text{b}}} - \frac{Q_{\text{m}}}{N_{\text{b}}} \right) - \sigma_{\ell\text{v}}, \quad (5)$$

where Q_{s} is the energy of sublimation per molecule and N_{b} is the number of the bonds per molecule in the crystal [22]. For snow crystals, we know that $\rho_{(10\bar{1}0)} > \rho_{(0001)}$, from consideration of the surface molecular structures of ice, and $Q_{\text{s}} > Q_{\text{m}}$, from experimental tables [22]. Thus $\Delta\sigma_{(10\bar{1}0)} > \Delta\sigma_{(0001)}$. According to Eqs.(3) and (4), this implies that the quasi-liquid layer on a face $(10\bar{1}0)$ remains at lower temperature than that on a face (0001) . Thus snow crystals have the following four different surface structures [11]: (I) both the

faces $(10\bar{1}0)$ and (0001) are covered with a quasi-liquid layer; (II) the face $(10\bar{1}0)$ is covered with a quasi-liquid layer, while the face (0001) has no quasi-liquid layer and is rough at the molecular level; (III) neither has a quasi-liquid layer, but $(10\bar{1}0)$ is rough, while (0001) is smooth at the molecular level; (IV) neither has a quasi-liquid layer, and both are smooth at the molecular level. These structural differences result in differences in the growth speeds of these faces, since the mechanisms governing the growth depend on the surface structures. Assuming that the first surface structure transforms into the second at -4°C , the second transforms into the third at -10°C , and the third transforms into the fourth at -22°C , Kuroda and Lacmann succeeded in describing the three crystal form transitions in the phase diagram [11].

The above consideration regards only the surface structures of faces. The situation becomes more interesting when we also consider the surface structures of the edges and vertices. There exhibit transitions that differ from those of the basal and prism faces, as we shown in the following section.

III. QUASI-LIQUID ON THE EDGES AND VERTICES OF SNOW CRYSTALS

First, we approximate the energetic advantage represented by the surface melting parameter for the edges and the vertices of snow crystals, $\Delta\sigma_{(\text{edge \& vertex})}$. In the process of snow crystal formation, the edges and vertices are formed as the intersections of metastable and unstable faces, such as $(11\bar{2}0)$, $(10\bar{1}1)$ and $(11\bar{2}1)$. For this reason, we approximate $\Delta\sigma_{(\text{edge \& vertex})}$ by taking the average of $\Delta\sigma$ for the intersecting faces. It is known from the molecular structure of ice that these metastable and unstable faces are rough and have large broken bond densities in comparison with the faces (0001) and $(10\bar{1}0)$. Thus, from Eq.(5), we see that $\Delta\sigma_{(\text{edge \& vertex})}$ is much larger than $\Delta\sigma_{(0001)}$ and $\Delta\sigma_{(10\bar{1}0)}$:

$$\Delta\sigma_{(0001)} < \Delta\sigma_{(10\bar{1}0)} < \Delta\sigma_{(\text{edge \& vertex})}. \quad (6)$$

This implies that for the edges and vertices, it is more energetically advantageous to have a surface transition from solid to liquid, and thus that they have a greater affinity for quasi-liquid. It is suggested by Eqs.(3) and (4) that there exists quasi-liquid on the edges and vertices at lower temperatures than on the faces (0001) and $(10\bar{1}0)$.

In Fig.2, we present surface structures of snow crystals in which the quasi-liquid of the

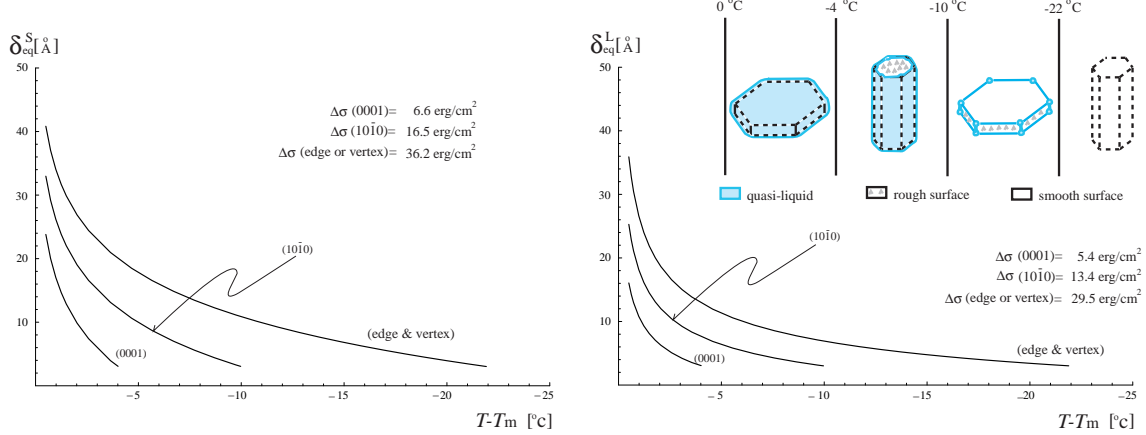


FIG. 2: The equilibrium thickness of a quasi-liquid layer for $W^S(\delta)$ and $W^L(\delta)$ as functions of temperature for various surface orientations. We chose $A = 10 \text{ \AA}$, corresponding to the characteristic coherence length of a water molecule in the quasi-liquid [9]. This is also the cluster size in water [25]. The quantity $\Delta\sigma$ is computed using the monolayer thickness (3 \AA) at -4°C , -10°C and -22°C . (From Eq.(5), we obtain $\Delta\sigma(0001) = 31 \text{ erg/cm}^2$, $\Delta\sigma(10\bar{1}0) = 37 \text{ erg/cm}^2$ and $\Delta\sigma(11\bar{2}0) = 54 \text{ erg/cm}^2$, where we use experimental values $\sigma_{\ell v} = 76 \text{ erg/cm}^2$ at 0°C , $Q_s = 8.48 \times 10^{-13} \text{ erg/molecule}$, and $Q_m = 1.0 \times 10^{-13} \text{ erg/molecule}$ [11]. These values of $\Delta\sigma$ are not accurate, because σ_{vs} for an actual relaxed vapor-solid interface is less than $\rho Q_s / (2N_B)$ for a freshly cut surface [22]. Also, for actual values of $\sigma_{s\ell}$, we must take into account the fact that the water-ice interface has a diffuse structure throughout the thickness of several molecular layers [20]. However, it is certain that $\Delta\sigma(0001) < \Delta\sigma(10\bar{1}0) < \Delta\sigma(\text{edge \& vertex})$.)

edges and vertices are taken into account. We find the following: (I) from 0°C to -4°C , all the faces, edges and vertices are covered with quasi-liquid; (II) from -4°C to -10°C , the faces $(10\bar{1}0)$, edges and vertices are covered with quasi-liquid, while the faces (0001) have no quasi-liquid and are rough; (III) from -10°C to -22°C , the edges and vertices are covered with quasi-liquid, while the faces (0001) are smooth and the faces $(10\bar{1}0)$ are rough, both without quasi-liquid; (IV) below -22°C , no quasi-liquid exists. In the following sections, we examine the stability of the quasi-liquids on the edges and vertices in a vapor environment.

IV. QUASI-LIQUID LAYER ON A CURVED SOLID SURFACE

To investigate the curvature effect on quasi-liquid at the edges and vertices, we consider here three- and two-dimensional ice particles covered with quasi-liquid[26]. We assume that the particles are in a vapor environment and have radius $h + \delta$, where h is the radius of the solid core and δ is the thickness of the quasi-liquid layer. Although the main reason we consider this system is to examine curvature effects on a quasi-liquid, the system itself has meaning as a model of ice nucleation in a vapor environment.

We assume a free energy of the above described system as

$$\Delta G_{\text{particle}}(h, \delta) = 2^{D-1}\pi \left[h^{D-1}(\sigma_{s\ell} + \Delta\sigma W(\delta)) + (h + \delta)^{D-1}\sigma_{\ell v} - \frac{1}{D} \left\{ (h + \delta)^D - h^D \right\} \frac{\mu_v - \mu_\ell}{V_q} - \frac{1}{D} h^D \frac{\mu_v - \mu_s}{V_s} \right], \quad (7)$$

where $D = 3$ for three-dimensional particles and $D = 2$ for two-dimensional particles, μ_v , μ_ℓ and μ_s are the chemical potentials per molecule for the bulk vapor, bulk liquid and bulk solid, and V_q and V_s are the volumes per molecule for the quasi-liquid and the solid. The first two terms on the right-hand side of Eq.(7) are the surface energies of the system, and the last two terms are the bulk contributions. The surface energy contribution must coincide with $2^{D-1}\pi h^{D-1}\sigma_{vs}$ for $\delta = 0$ and $2^{D-1}\pi h^{D-1}\sigma_{s\ell} + 2^{D-1}\pi(h + \delta)^{D-1}\sigma_{\ell v}$ for $\delta \rightarrow \infty$. Thus $W(0) = 1$ and $W(\infty) = 0$. As in Eq.(2), we use two types of $W(\delta)$: $W_S(\delta) = \exp(-\delta/A)$ and $W_L(\delta) = (1 + \delta/A)^{-2}$. The quantity $\Delta G_{\text{particle}}(h, \delta)/(2^{D-1}\pi h^{D-1})$ reduces to Eq.(2) when $\mu_v = \mu_s$ and $h \rightarrow \infty$. Since we are interested in the growth of ice in a vapor environment, we assume $\mu_v > \mu_s$ and $\mu_\ell > \mu_s$ in the following.

The equilibrium condition is given by the equations

$$\frac{\partial \Delta G_{\text{particle}}}{\partial \delta} = 0, \quad (8)$$

$$\frac{\partial \Delta G_{\text{particle}}}{\partial h} = 0. \quad (9)$$

In equilibrium, we find a useful relation between δ and h . From Eq.(8), we have

$$(D - 1)(h + \delta)^{D-2}\sigma_{\ell v} - (h + \delta)^{D-1} \frac{\mu_v - \mu_\ell}{V_q} = -h^{D-1} \Delta\sigma \frac{dW(\delta)}{d\delta}. \quad (10)$$

Thus, Eq.(9) becomes

$$(D - 1)W(\delta) - h \frac{dW(\delta)}{d\delta} = \frac{h}{\Delta\sigma} \left(\frac{\mu_v - \mu_s}{V_s} - \frac{\mu_v - \mu_\ell}{V_q} - \frac{(D - 1)\sigma_{s\ell}}{h} \right). \quad (11)$$

This equation determines δ as a function of h . If we use $W(\delta) = W_S(\delta)$, we obtain

$$\delta^S(h) = -A \ln \left[\frac{h}{(D-1)A + h} \right] - A \ln \left[\frac{A\lambda(h)}{\Delta\sigma} \right], \quad (12)$$

and if we use $W(\delta) = W_L(\delta)$, we obtain

$$\delta^L(h) = -A + A \left(\chi(h, \lambda(h)) + \frac{(D-1)\Delta\sigma}{3h\lambda(h)} \frac{1}{\chi(h, \lambda(h))} \right), \quad (13)$$

where $\lambda(h)$ and $\chi(h, \lambda)$ are defined by

$$\lambda(h) = \frac{\mu_\ell - \mu_s}{V_q} + \left(\frac{1}{V_s} - \frac{1}{V_q} \right) (\mu_v - \mu_s) - \frac{(D-1)\sigma_{s\ell}}{h}, \quad (14)$$

and

$$\chi(h, \lambda) = \left\{ \frac{\Delta\sigma}{A\lambda} \left(1 + \sqrt{1 - \frac{(D-1)^3 A^2 \Delta\sigma}{27h^3 \lambda}} \right) \right\}^{\frac{1}{3}}. \quad (15)$$

The above functions $\delta^S(h)$ and $\delta^L(h)$ diverge at $h = h_c \equiv (D-1)\sigma_{s\ell} / \{(\mu_v - \mu_s)/V_s - (\mu_v - \mu_\ell)/V_q\}$, and when $h > h_c$, they monotonically decrease and approach the following $\delta^S(\infty)$ and $\delta^L(\infty)$ asymptotically:

$$\delta^S(\infty) = -A \ln \left[\frac{A\lambda(\infty)}{\Delta\sigma} \right], \quad (16)$$

$$\delta^L(\infty) = -A + \left(\frac{2A^2 \Delta\sigma}{\lambda(\infty)} \right)^{\frac{1}{3}}. \quad (17)$$

No real solution of $\delta^S(h)$ and $\delta^L(h)$ exists for $0 < h < h_c$.

When $V_s > V_q$, which holds for ice and water (and quasi-liquid), the following relations hold:

$$h_c > (D-1)V_s\sigma_{s\ell}/(\mu_\ell - \mu_s), \quad \delta^S(\infty) > \delta_{\text{eq}}^S, \quad \delta^L(\infty) > \delta_{\text{eq}}^L. \quad (18)$$

The quantities δ_{eq}^S and δ_{eq}^L are given in Eqs.(3) and (4). Thus we find the following two properties of h and δ . One is that $h > (D-1)V_s\sigma_{s\ell}/(\mu_\ell - \mu_s)$ in equilibrium. For $D = 3$, this means that the equilibrium radius of the solid part of the particle, h , is always larger than the critical radius of ice nucleation in supercooled water. The other is that $\delta^S(h)$ in Eq.(12) and $\delta^L(h)$ in Eq.(13) are always greater than δ_{eq}^S in Eq.(3) and δ_{eq}^L in Eq.(4), respectively. This implies that the equilibrium thickness δ on a curved surface is greater than that on a plane surface, δ_{eq} .

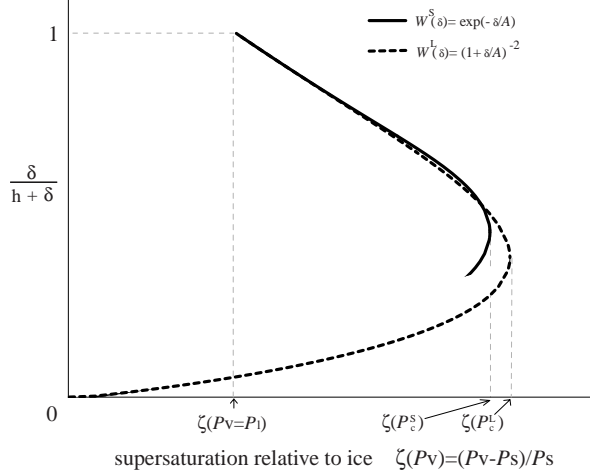


FIG. 3: The equilibrium states of a quasi-liquid on a curved surface as a function of the supersaturation relative to ice. For this figure, we set $T = -15^\circ\text{C}$, $\Delta\sigma = 36.2 \text{ erg/cm}^2$, $A = 10 \text{ \AA}$ and $V_q = V_s = 30 \text{ \AA}^3$. From experimental values for water and ice, we have $\sigma_{s\ell} = 24.25 \text{ erg/cm}^2$ and $\sigma_{\ell v} = 78.25 \text{ erg/cm}^2$ at -15°C [22].

We solved Eqs.(8) and (9) numerically. In Fig.3, we plot the ratio $\delta/(h+\delta)$ in equilibrium as a function $(P_v - P_s)/P_s$, where P_v is the actual vapor pressure and P_ℓ and P_s are the equilibrium vapor pressures for the bulk liquid and the bulk solid, respectively. To obtain Fig.3, we have used the relations

$$\mu_v(T, P_v) = \mu_v(T) + kT \ln P_v, \quad (19)$$

$$\mu_\ell(T, P_\ell) = \mu_v(T, P_\ell) = \mu_v(T) + kT \ln P_\ell, \quad (20)$$

$$\mu_s(T, P_s) = \mu_v(T, P_s) = \mu_v(T) + kT \ln P_s, \quad (21)$$

where k is the Boltzmann constant and $\mu_v(T)$ is the chemical potential of vapor at $P_v = 1$. When $P_\ell > P_v > P_s$, the equilibrium state is uniquely determined. When $P_v \geq P_\ell$, in addition to this state, another equilibrium state that has a thicker quasi-liquid layer appears. This state appears because above P_ℓ it is possible not only for the solid but also for the liquid to grow in the vapor environment. As the supersaturation P_v increases, these two equilibrium states approach each other, and at $P_v = P_c$ they coincide. Above P_c no equilibrium state exists. All the equilibrium states obtained here are labile equilibrium states. From the viewpoint of ice nucleation in a vapor environment, they all correspond to a critical radius of nucleation.

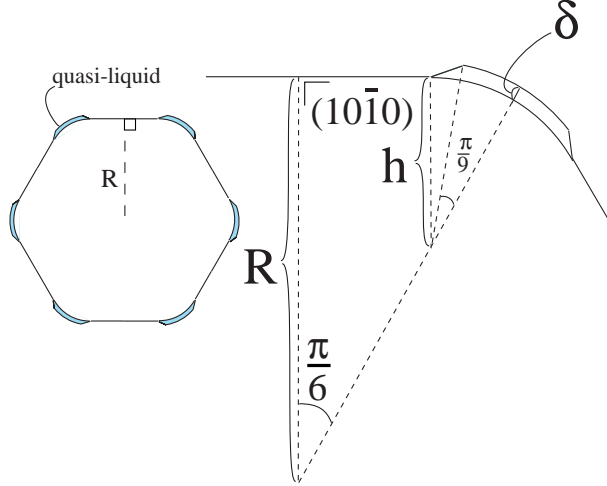


FIG. 4: The quasi-liquid remaining on an edge.

V. INSTABILITY OF THE QUASI-LIQUID REMAINING ON THE EDGE OF THE CRYSTAL

Let us now consider a snow crystal whose edges are covered with quasi-liquid and whose faces have no quasi-liquid layer (see Fig.2). For the sake of simplicity, we consider only the six edges at which two different prism faces meet (see fig.4). For other edges and vertices, similar analyses can be carried out and yield qualitatively similar results.

The six prism faces $(10\bar{1}0)$ grow slowly in comparison with the edges, and therefore we use the approximation that their speed of growth is zero. As shown in Fig.4, we also simplify the shape of the quasi-liquid layer on the edges. This simplification is justified when $\delta < h$. For this system, the free energy of the snow crystal is given as

$$\begin{aligned} \Delta G_{\text{prism}}(h, \delta)/12 = & \left[\frac{R}{\sqrt{3}}\sigma_{(10\bar{1}0)} - \frac{R^2}{2\sqrt{3}}\frac{\mu_v - \mu_s}{V_s} \right] - \left[\frac{h}{\sqrt{3}}\sigma_{(10\bar{1}0)} - \frac{h^2}{2\sqrt{3}}\frac{\mu_v - \mu_s}{V_s} \right] \\ & + \left[\frac{\pi}{6}h(\sigma_{sl(\text{edge})} + \Delta\sigma_{(\text{edge})}W(\delta)) \right. \\ & + \left. \left\{ \frac{\pi}{9}(h + \delta) + \sqrt{h^2 + (h + \delta)^2 - 2h(h + \delta)\cos\left(\frac{\pi}{18}\right)} \right\} \sigma_{\ell v} \right. \\ & \left. - \left\{ \frac{\pi}{18}((h + \delta)^2 - h^2) + \frac{1}{2}\left(h(h + \delta)\sin\left(\frac{\pi}{18}\right) - \frac{\pi}{18}h^2\right) \right\} \frac{\mu_v - \mu_\ell}{V_q} - \frac{\pi}{12}h^2\frac{\mu_v - \mu_s}{V_s} \right], \quad (22) \end{aligned}$$

where $\sigma_{(10\bar{1}0)}$ is the surface energy for a prism face that has no quasi-liquid layer and adsorbs H_2O molecules, and $\sigma_{sl(\text{edge})}$ and $\Delta\sigma_{(\text{edge})}$ are the surface energy of the solid-liquid interface and the energetic advantage of surface melting (given by Eq.(5)) for the surface of the edge,

respectively. The curvature effects considered in the previous section are taken into account by the terms inside the last set of square brackets on the right-hand side of Eq.(22). When $h > \delta$ and $(\frac{\delta}{h})^3 \sim 0$, Eq.(22) becomes

$$\begin{aligned} \Delta G_{\text{prism}}(h, \delta)/12 = & \left[\frac{R}{\sqrt{3}} \sigma_{(10\bar{1}0)} - \frac{R^2}{2\sqrt{3}} \frac{\mu_v - \mu_s}{V_s} \right] - \left[\frac{h}{\sqrt{3}} \sigma_{(10\bar{1}0)} - \frac{h^2}{2\sqrt{3}} \frac{\mu_v - \mu_s}{V_s} \right] \\ & + \left[\frac{\pi}{6} h (\sigma_{s\ell(\text{edge})} + \Delta\sigma_{(\text{edge})} W(\delta)) \right. \\ & + \frac{\pi}{9} \left\{ (h + \delta) + \frac{1}{2} \left\{ 1 + \frac{\delta}{2h} + \frac{1}{4} \left\{ \left(\frac{\pi}{36} \right)^{-2} - 1 \right\} \left(\frac{\delta}{h} \right)^2 \right\} h \right\} \sigma_{\ell v} \\ & \left. - \frac{\pi}{36} (2\delta^2 + 5h\delta) \frac{\mu_v - \mu_\ell}{V_q} - \frac{\pi}{12} h^2 \frac{\mu_v - \mu_s}{V_s} \right], \end{aligned} \quad (23)$$

where

$$\begin{aligned} \sqrt{h^2 + (h + \delta)^2 - 2h(h + \delta) \cos\left(\frac{\pi}{18}\right)} &= \sqrt{\delta^2 + 4h(h + \delta) \sin^2\left(\frac{\pi}{36}\right)} \\ &\simeq 2 \sin\left(\frac{\pi}{36}\right) h \left\{ 1 + \frac{\delta}{2h} + \frac{1}{4} \left(\sin^{-2}\left(\frac{\pi}{36}\right) - 1 \right) \left(\frac{\delta}{h} \right)^2 \right\}, \end{aligned}$$

and we have used the approximations $\sin\left(\frac{\pi}{18}\right) \simeq \frac{\pi}{18}$ and $\sin\left(\frac{\pi}{36}\right) \simeq \frac{\pi}{36}$. The equilibrium condition is given by

$$\frac{\partial \Delta G_{\text{prism}}}{\partial \delta} = 0, \quad (24)$$

$$\frac{\partial \Delta G_{\text{prism}}}{\partial h} = 0. \quad (25)$$

From Eq.(25), we find

$$h = h_0 = \frac{\frac{1}{\sqrt{3}} \sigma_{(10\bar{1}0)} - \frac{\pi}{6} \sigma_{\text{vs}(\text{edge})}}{\left(\frac{1}{\sqrt{3}} - \frac{\pi}{6} \right) \frac{\mu_v - \mu_s}{V_s}}, \quad (26)$$

where $\sigma_{\text{vs}(\text{edge})}$ is the surface energy of the vapor-solid interface for the edge. In order for h_0 to be positive (which means that the curved edge is energetically stable) and for $\left(\frac{\partial \Delta G_{\text{prism}}}{\partial \delta} \right)_{\delta=0}^{h=h_0} < 0$ to hold (which means that a curved edge with a quasi-liquid layer is energetically stable), $\sigma_{(10\bar{1}0)}$ must satisfy

$$\sigma_{(10\bar{1}0)} > \frac{\sqrt{3}\pi}{6} \sigma_{\text{vs}(\text{edge})} + \frac{\frac{5}{6} \left(\frac{1}{\sqrt{3}} - \frac{\pi}{6} \right) \sigma_{\ell v} \frac{\mu_v - \mu_s}{V_s}}{-\Delta\sigma_{(\text{edge})} \frac{\partial W(0)}{\partial \delta} + \frac{5}{6} \frac{\mu_v - \mu_\ell}{V_q}}. \quad (27)$$

This equation gives a lower bound on $\sigma_{(10\bar{1}0)}$.

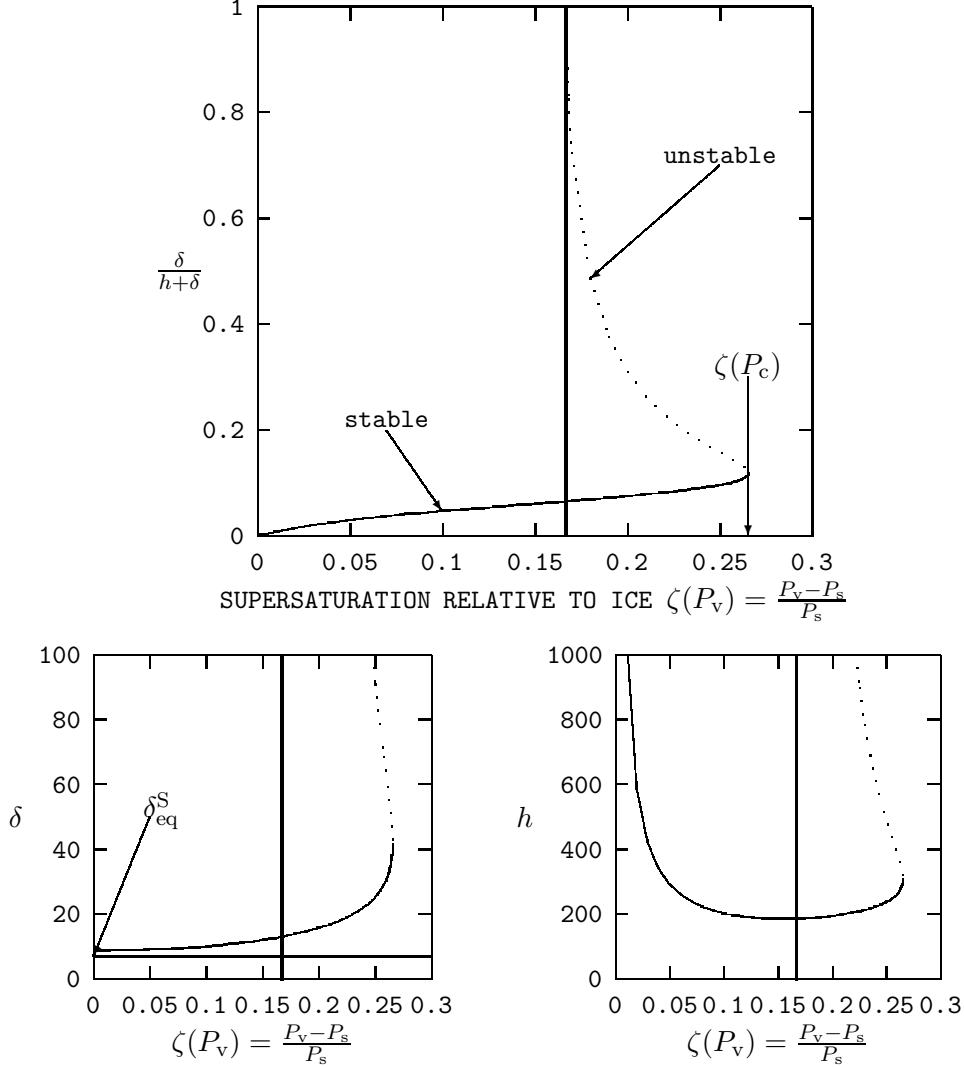


FIG. 5: The stability of the quasi-liquid remaining on an edge as a function of the supersaturation relative to ice. We plot the case of $W^S(\delta)$. For $W^L(\delta)$, qualitatively similar results are obtained. The vertical solid line at supersaturation 0.167 indicates the water saturation point. The horizontal line at δ_{eq}^S indicates the equilibrium thickness of a quasi-liquid layer on a planar surface, given by Eq.(3). We used $T = -15^\circ\text{C}$ (258.15K), $\sigma_{(10\bar{1}0)} = 129.82\text{erg/cm}^2$ and $\Delta\sigma_{(\text{edge})} = 36.2\text{erg/cm}^2$. We also used the experimental values at -15°C , $\sigma_{sl(\text{edge})} = 24.25\text{erg/cm}^2$ and $\sigma_{lv} = 78.25\text{erg/cm}^2$ [22] (and therefore $\sigma_{vs(\text{edge})} = 138.7\text{erg/cm}^2$). This model is justified when δ is larger than the mono-layer thickness and h is sufficiently large. Thus we ignore the unstable solutions existing for $\delta < 3 \text{ \AA}$ and $h < 30 \text{ \AA}$. This type of figure can be obtained when $\sigma_{(10\bar{1}0)} > 128.9\text{erg/cm}^2$. When $\mu_v - \mu_s \rightarrow \infty$, the right-hand side of Eq.(27) converges to 133.07 erg/cm^3 . This value is reasonable for a rough face $(10\bar{1}0)$ having no quasi-liquid layer. (c.f. $\sigma_{vs(10\bar{1}0)} = \rho Q_s / (2N_B) = 128\text{erg/cm}^2$, where $Q_s = 8.5 \times 10^{-13}\text{erg/molecule}$). The critical supersaturation $\zeta(P_c)$ is 0.265.

Numerical solutions of Eqs.(24) and (25) are plotted in Fig.5. (Here we have used Eqs.(19)-(21) again.) Remarkably, we find a stable equilibrium state when $P_v < P_c$. In this case, a snow crystal with small δ and h evolves toward a stable state, at which point it ceases growing.

When $P_v > P_c$ ($> P_\ell$), no stable solution satisfying Eqs.(24) and (25) is found. It is interesting that the thickness δ continues to grow in this case. This suggests that a novel instability arises on the edges of snow crystals when $P_v > P_c$. Of course, in a real system, δ cannot continue to grow indefinitely, and thus this result reveals a limitation of our model. Our model breaks down when δ becomes comparable with h , and our simplification regarding the shapes of the quasi-liquids on the edges is no longer justified. In a real system, as the thickness of the quasi-liquid grows, eventually it begins overflowing onto the neighboring faces $(10\bar{1}0)$ or (0001) to reduce the surface energy. We interpret the continuous growth of δ in our model as corresponding to the continuous overflowing of quasi-liquid in a real system. If the neighboring face is rough at the molecular level, the overflowing quasi-liquid sticks to the neighboring face, and immediately turns to be solid near the edge. As we show in the next section, this interpretation allows our model to explain the phase diagram of snow crystals.

VI. PHASE DIAGRAM

In this section we give a new description of the snow phase diagram. Let us reconsider the discussion of Section III. In the temperature regions (I), 0°C to -4°C , and (IV), below -22°C , the quasi-liquid on the edges and vertices does not play a special role. Thus we focus on the temperature regions (II) and (III), -4°C to -22° .

In the temperature region (II), -4°C to -10°C , the six prism faces $(10\bar{1}0)$, all the edges and all the vertices are covered with quasi-liquid, while the two basal faces (0001) are rough at the molecular level and have no quasi-liquid layers. As seen in Fig. 5, when the vapor pressure P_v is low, the quasi-liquids on the edges and vertices are stable. In this case, the edges and the vertices do not play a special role in the snow crystal formation. However, when P_v is higher than a certain value P_c ($> P_\ell$), the quasi-liquid on the edges and vertices overflows onto the neighboring faces. The quasi-liquid overflowing onto $(10\bar{1}0)$ spreads over the quasi-liquid layer, while the quasi-liquid overflowing onto rough (0001) sticks near the

edges and vertices and turns to solid. In this case, two types of overflow are possible. One is overflow from the vertices, and the other is overflow from the edges where the basal and prism faces meet. If the former becomes the main type of overflow, the resultant snow crystal should grow like a needle. If the latter becomes the main overflow according to our model, the resultant snow crystal should grow like a sheath.

In the temperature region (III), -10°C to -22°C , the edges and the vertices are covered with quasi-liquid, while the basal (0001) and prism ($10\bar{1}0$) faces possess no quasi-liquid layer. The basal faces are smooth and the prism faces are rough at the molecular level. Here again, as seen in Fig. 5, when P_v is low, the quasi-liquid is stable, and thus the snow crystal grows according to the theory of Kuroda and Lacmann. When P_v is higher than P_c ($> P_\ell$), the quasi-liquid overflows onto the neighboring faces. The quasi-liquid overflowing on to smooth (0001) spreads over (0001) and turns to solid, while the quasi-liquid overflowing onto rough ($10\bar{1}0$) sticks near the edges and vertices and turns to solid. In this case, three types of overflow are possible. The first is overflow from the vertices, the second is overflow from the edges where the basal and the prism faces meet, and the third is overflow from the edges where two prism faces meet. If the amounts of quasi-liquid involved in all overflows are of the same order, the resultant snow crystal should grow like a sector at about -10°C . If the first and (or) the third overflow are the main types of overflow, the resultant snow crystal should grow like a dendrite at about -15°C . Contrastingly if the first and (or) the third overflow are the main overflows, but the surface structure of prism face changes from a rough surface to a smooth surface with temperature falling, the resultant snow crystal should grow like a sector again. This is because the continuous overflow spreads over smooth prism faces and turns to solid successively. In this case, the overflow can act as a step source for prism faces and thus the snow crystal grows in the manner hypothesized by Frank [5] and found in the simulation of Yokoyama and Kuroda [6]. We believe that this type of sector can be observed at about -22°C .

We note that the critical supersaturation shown in Fig.5 is 0.265 at -15°C , which agrees with the experimental supersaturation, for which dendrites are observed above 0.20 (see Fig.1).

VII. SUMMARY

In this paper, we have shown theoretically that quasi-liquid layers exist on the edges and vertices of snow crystals between -4°C and -22°C , for which temperatures there is no quasi-liquid on the faces (0001) and $(10\bar{1}0)$.

To investigate the curvature effect on quasi-liquid layers at the edges and vertices, we considered an ice particle coated with a quasi-liquid layer, and derived the equilibrium over a range of supersaturation values. We found that below the water saturation point, the equilibrium state is uniquely determined. However, above this point, another equilibrium state exists because it is possible for bulk supercooled water to exist. Above the critical supersaturation point, no equilibrium state exists. We showed that the quasi-liquid layers for equilibrium states of a particle are thicker than the quasi-liquid layer for the equilibrium state of a planar surface.

Next, we considered a two-dimensional crystal. We found that there are temperatures for which the six prism faces possess no quasi-liquid, while the edges and vertices are covered with quasi-liquid. We have examined the stability of this system. We found that below the critical saturation, which is higher than the water saturation, the quasi-liquid layer exists in a stable state on the edges. However, above the critical supersaturation, the quasi-liquid becomes unstable, and continues to grow indefinitely. We interpret this indefinite growth as implying overflow onto the neighboring faces in a real system.

On the basis of our results, we have proposed a new description of snow crystal growth according to which the unstable growth of snow crystals, which prefer the edges and the vertices, is due to the overflow of the quasi-liquid from the edges and the vertices onto neighboring faces that are rough and have no quasi-liquid layers. We have shown that this overflowing occurs above the water saturation point and that these surface conditions of snow crystals are realized between -4°C and -22°C . This description naturally accounts the relation between the morphological instability and the water saturation in the snow phase diagram.

While we have succeeded in explaining the snow phase diagram qualitatively, for a more complete understanding, the details of crystal growth should be clarified by three-dimensional simulation. We also would like to show that secondary branches of the dendrites are produced by the overflow of quasi-liquid from the edges and vertices of the primary

branches. These are future problems.

In this paper, we have focused on the quasi-liquid of snow crystals. However surface melting is observed in many classes of solids, including metals, semiconductors, solid rare gases [21]. The model and method presented in this paper are also applicable to these materials, and should be useful for the investigation of general properties of surface melting.

Acknowledgments

Special thanks are due to Professor Y. Furukawa and M. Sato for many fruitful discussions.

-
- [1] U. Nakaya, Compendium of Meteorology, edited by T. F. Malone (American Meteorological Society, Boston, 1951), p.207 ; Snow Crystals-Natural and Artificial (Harvard University Press, Cambridge, MA, 1954).
 - [2] H. J. Aufm Kampe, H. K. Weickmann, and J. J. Kelly, *J. Metals* **8**, 168 (1951); J. Hallet and B. J. Mason, *Proc. R. Soc. (London)* **A247**, 440 (1958); T. Kobayashi, *Phil. Mag.* **6**, 1363 (1961).
 - [3] D. Lamb and P. V. Hobbs, *J. Atmos. Sci.* **28**, 1506 (1971).
 - [4] W. K. Burton and N. Cabrera, *Disc. Faraday Soc.* **5** 33, 40 (1949); W. K. Burton, N. Cabrera and F. C. Frank, *Phil. Trans. Roy. Soc.* **A243**, 299 (1950 ~ 1951).
 - [5] F. C. Frank, *J. Cryst. Growth* **24/25**, 3 (1974).
 - [6] E. Yokoyama and T. Kuroda, *Phys. Rev.* **A41**, 2038 (1990).
 - [7] M. Faraday, *Phil. Mag.* **17**, 162 (1859).
 - [8] W. A. Weyl, *J. Coll. Sci.* **6**, 389 (1951).
 - [9] N. H. Fletcher, *Phil. Mag.* **7**, 255 (1962) ; **8**, 1425 (1963) ; **18**, 1287 (1968).
 - [10] R. Lacmann and I. N. Stranski, *J. Cryst. Growth* **13/14**, 236 (1972).
 - [11] T. Kuroda and R. Lacmann *J. Cryst. Growth* **56**, 189 (1982).
 - [12] T. Kuroda, *J. Crystal Growth*, 99, 83 (1990).
 - [13] V. I. Kvlividze, V. F. Kiselev, A. B. Kuraev and L. A. Ushakova, *Surf. Sci.* **44**, 60 (1974).
 - [14] Y. Mizuno, and N. Hanafusa, *J. Phys. Coll.* **48**, C1 (1987).
 - [15] D. Beaglehole, and D. Nason, *Surf. Sci.* **96**, 357 (1980).

- [16] Y.Furukawa, M.Yamamoto and T.Kuroda, *J. Cryst. Growth* **82**, 665 (1987).
- [17] I. Goleki, and C. J. Jaccard, *Phys. Lett. A***63**, 374 (1977).
- [18] A. Lied, H. Dosch, and J. H. Bilgram, *Phys. Rev. Lett.* **72**, 3554 (1994) ; *Surf. Sci.* **327**, 145 (1995) ; *Surf. Sci* **366**, 43 (1996).
- [19] M. Elbaum, *Phys. Rev. Lett.* **67**, 2982 (1991); M. Elbaum, S. G. Lipson and J. G. Dash, *J. Cryst. Growth* **129**, 491 (1993).
- [20] H. Nada and Y. Furukawa *Jpn. J. Appl. Phys.* **34**, 583 (1995); *J. Cryst. Growth* **169**, 587 (1996); *J. Phys. Chem.* **B101**, 6163 (1997).
- [21] J. G. Dash, Haiying Fu and J. S. Wettlaufer, *Rep. Prog. Phys.* **58**, 115(1995).
- [22] *Microphysics of Clouds and Precipitation* by Hans R. Pruppacher and James D. Klett (Kluwer Academic Publishers).
- [23] M. B. Baker and J. G. Dash, *J. Cryst. Growth* **97**, 770 (1989).
- [24] D. Nenow and A. Trayanov, *J. Cryst.Growth* **99**, 102 (1990).
- [25] D. Nenow, *Prog. Cryst. Growth Charact.* **9**, 185 (1984).
- [26] Other curvature models of surface melting are presented in Refs. [23] and [24].